

# Regulatory Strategies in the Complexation and Release of a Noncovalent Guest Trimer by a Self-Assembled Molecular Cage\*\*

Jessica M. C. A. Kerckhoffs, Fijis W. B. van Leeuwen, Anthony L. Spek, Huub Kooijman, Mercedes Crego-Calama,\* and David N. Reinhoudt\*

Self-assembly,<sup>[1]</sup> nowadays recognized as one of the most promising techniques for building nanoscale structures,<sup>[2]</sup> is nature's favorite way of building objects, probably because it is the most economic and reliable strategy. Life is made possible by highly complex functional structures built with great perfection by self-assembly, which allows for errors to be minimized and/or spontaneously corrected.<sup>[3]</sup> The same supramolecular principles have made it possible to assemble synthetic building blocks into predictable assemblies.<sup>[4]</sup> However, the organizational complexity and control found in biological structures for the creation of recognition sites is still far beyond the ability of chemists. Building complex synthetic structures with specific function through self-assembly remains a challenge.<sup>[5]</sup> One of the more intriguing aspects of biological and chemical self-assembly is the capture and organization of guest molecules in self-assembled cages and capsules.<sup>[6]</sup> The entrapment of guest molecules in synthetic self-assembled systems is mainly achieved by steric constraints in rigid preorganized building blocks. Bulky solvents that cannot occupy the cavities are used for efficient encapsulation of guests. There are few examples where the self-organization of the enclosure occurs through noncovalent interactions.<sup>[7]</sup> Furthermore, supramolecular systems with higher hierarchy of assembly in both the host and guest obtained through the use of the same type of noncovalent interactions were until now unknown.

Here we report a dynamic self-assembled system where the reversibility of the association allows changes in the constitution by all of the most characteristic processes of supramolecular chemistry, namely, internal rearrangement,

[\*] Dr. M. Crego-Calama, Prof. D. N. Reinhoudt, Dr. J. M. C. A. Kerckhoffs, F. W. B. van Leeuwen  
Laboratory of Supramolecular Chemistry and Technology  
MESA<sup>+</sup> Research Institute, University of Twente  
P.O. Box 217, 7500 AE Enschede (The Netherlands)  
Fax: (+31) 534-894-645  
E-mail: m.crego-calama@ct.utwente.nl  
d.n.reinhoudt@ct.utwente.nl

Prof. A. L. Spek, Dr. H. Kooijman  
Department of Crystal and Structural Chemistry  
Bijvoet Center for Biomolecular Research, Utrecht University  
Padualaan 8, 3584 CH Utrecht (The Netherlands)

[\*\*] This work has been financially supported in part by the Technology Foundation of the Netherlands (J.M.C.A.K.) and the Council for Chemical Sciences of the Netherlands Organization for Scientific Research (CW-NOW to A.L.S.). The research of M.C.-C. has been made possible by a fellowship from the Royal Netherlands Academy of Arts and Sciences.

incorporation, exchange, and extrusion of components.<sup>[8]</sup> More specifically, we describe here the template-assisted assembly of a hydrogen-bonded trimer inside a molecular cage that itself is also assembled through the formation of hydrogen bonds.<sup>[9]</sup> Remarkably, this self-assembled receptor shows some primitive similarities with regulatory strategies of natural systems such as enzymes and viruses.<sup>[3b]</sup> The self-assembled receptor has the ability to adapt its geometry to that of the guest trimer by undergoing large conformational changes. Furthermore, the receptor has the capacity to release the encapsulated material when it receives a specific external molecular signal.

Recently, we have exploited the circular network (rosette)<sup>[10]</sup> of complementary hydrogen bonds formed between melamine and barbituric (BAR) or 1,3,5-triazine-2,4,6-triol (cyanuric acid, CYA) for the noncovalent synthesis of self-assembled nanometer-sized molecular boxes,  $1_3 \cdot (\text{DEB})_6$  (DEB = diethylbarbituric acid) or  $1_3 \cdot (\text{BuCYA})_6$  (BuCYA = butylcyanuric acid), respectively.<sup>[11]</sup> The assemblies are formed spontaneously through the formation of 36 cooperative hydrogen bonds by mixing calix[4]arene dimelamines **1** with either two equivalents of barbiturates or cyanurates in apolar solvents such as chloroform, toluene, or benzene. These thermodynamically highly stable molecular boxes consist of two flat rosette motifs connected through three calix[4]arene moieties (Figure 1).

During the course of our studies on these self-assembled nanostructures as potential mimics for antibodies<sup>[12]</sup> we

identified a complex  $1a_3 \cdot (\text{DEB})_6 \cdot 2_3$  in which the hydrogen-bonded molecular box  $1a_3 \cdot (\text{DEB})_6$  encapsulates the also hydrogen-bonded alazarine trimer **2**, both in organic solvents and in the solid state. Besides the formation of the complex, we were able to elucidate, by a combination of X-ray and <sup>1</sup>H NMR studies, the conformational changes experienced by the molecular box  $1a_3 \cdot (\text{DEB})_6$  upon encapsulation and release of **2**.

Crystallization of assembly  $1a_3 \cdot (\text{DEB})_6 \cdot 2_3$  by diffusion of hexane into a solution of the complex in dichloromethane gave cubic red/orange crystals (0.25–1 mm).<sup>[13]</sup> The X-ray crystallographic analysis (Figure 2) revealed that the space between the two rosette layers is filled by a layer of three coplanar alazarine molecules that are interlocked by an array of hydrogen bonds, with the OH groups in the alazarine (**2**) pointing outwards from the threefold rotation axis of the complex. The O...O distance (between the carbonyl group of one guest molecule and the hydroxy group of the adjacent guest molecule) in the hydrogen-bonded network forming the **2**<sub>3</sub> trimer is 2.7 Å, which is within the distance for the formation of a hydrogen bond. Furthermore, the crystal structure reveals that the two melamine units of one calix[4]arene molecule are in an eclipsed orientation, thus inferring that the complex  $1a_3 \cdot (\text{DEB})_6 \cdot 2_3$  has *C*<sub>3h</sub> symmetry (Figure 1b). In this way the electron-deficient aromatic ring of **2** is stacked in between the two relatively electron poor aromatic rings of the melamine unit, thus maximizing the π–π interactions.<sup>[14]</sup> The eclipsed orientation adopted by the

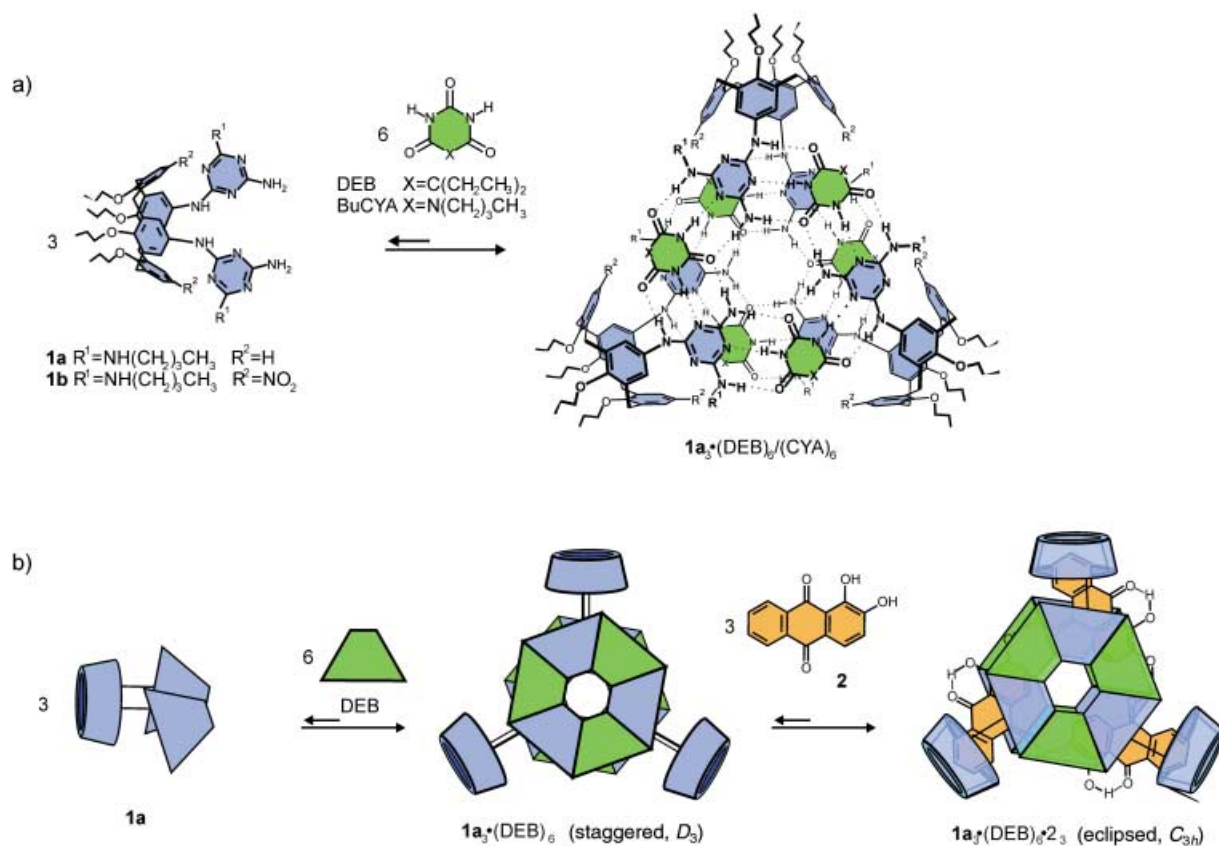


**Figure 1.** a) Self-assembly of  $1_3 \cdot (\text{DEB})_6 / (\text{CYA})_6$ . b) Schematic representation of the formation of  $1a_3 \cdot (\text{DEB})_6$  and  $1a_3 \cdot (\text{DEB})_6 \cdot 2_3$  showing the rearrangement of the double rosette  $1a_3 \cdot (\text{DEB})_6$  from a staggered to an eclipsed conformation after encapsulation of **2**.

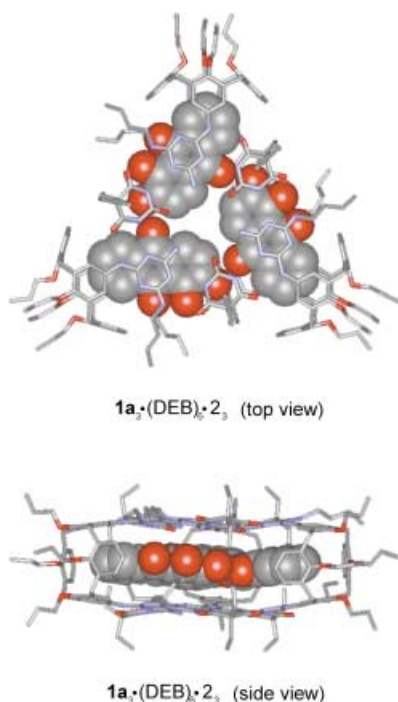


**Figure 2.** Top and side view of the crystal structure of the complex  $1\mathbf{a}_3 \cdot (\text{DEB})_6 \cdot 2_3$  (a space-filling model representation for the trimer  $2_3$  and a stick model for the molecular box,  $1\mathbf{a}_3 \cdot (\text{DEB})_6$ ). Only the main component of the disordered butyl and propyl groups are shown. Hydrogen atoms are not shown for clarity.

melamine units in the solid state is surprising because, as demonstrated by X-ray and  $^1\text{H}$  NMR spectroscopy,<sup>[11]</sup> empty assemblies of type  $1_3 \cdot (\text{DEB})_6$  are formed exclusively as the staggered isomer with a  $D_3$  symmetry.

Other important structural information can be extracted by comparing the crystal structure of the complex  $1\mathbf{a}_3 \cdot (\text{DEB})_6 \cdot 2_3$  with that of the empty double rosette  $1\mathbf{b}_3 \cdot (\text{DEB})_6$ .<sup>[11b]</sup> In the empty assembly  $1\mathbf{b}_3 \cdot (\text{DEB})_6$ , the two rosette layers are practically stacked on top of each other with an intermolecular separation of 3.5 Å at the edges and 3.2 Å in the center, while the crystal structure of  $1\mathbf{a}_3 \cdot (\text{DEB})_6 \cdot 2_3$  reveals that the intermolecular separation between the two rosette layers increases to 6.7 Å at the edges and to 6.4–6.9 Å at the center upon encapsulation of  $2_3$  (Figure 3). This very efficient structural regulation is possible because of the impressive structural flexibility of the calix[4]arene platform.

These structural changes suggest that the two rosette floors in the self-assembled nanostructure  $1\mathbf{a}_3 \cdot (\text{DEB})_6$  undergo some sort of allosteric regulation upon encapsulation of the guest. In the resulting structure the two rosette floors, as defined by the barbiturates, move apart 3.0–3.5 Å and turn 60° (from staggered to eclipsed) in the formation of the  $1\mathbf{a}_3 \cdot (\text{DEB})_6 \cdot 2_3$  complex. This ability to transmit conformational changes between spatially distinct sites within this “super”-structure is possible because of the inherent dynamic character of the self-assembled structures.

Such regulatory strategies occur widely in nature.<sup>[3b]</sup> For example, the catalytic trimers in aspartate transcarbamoylase

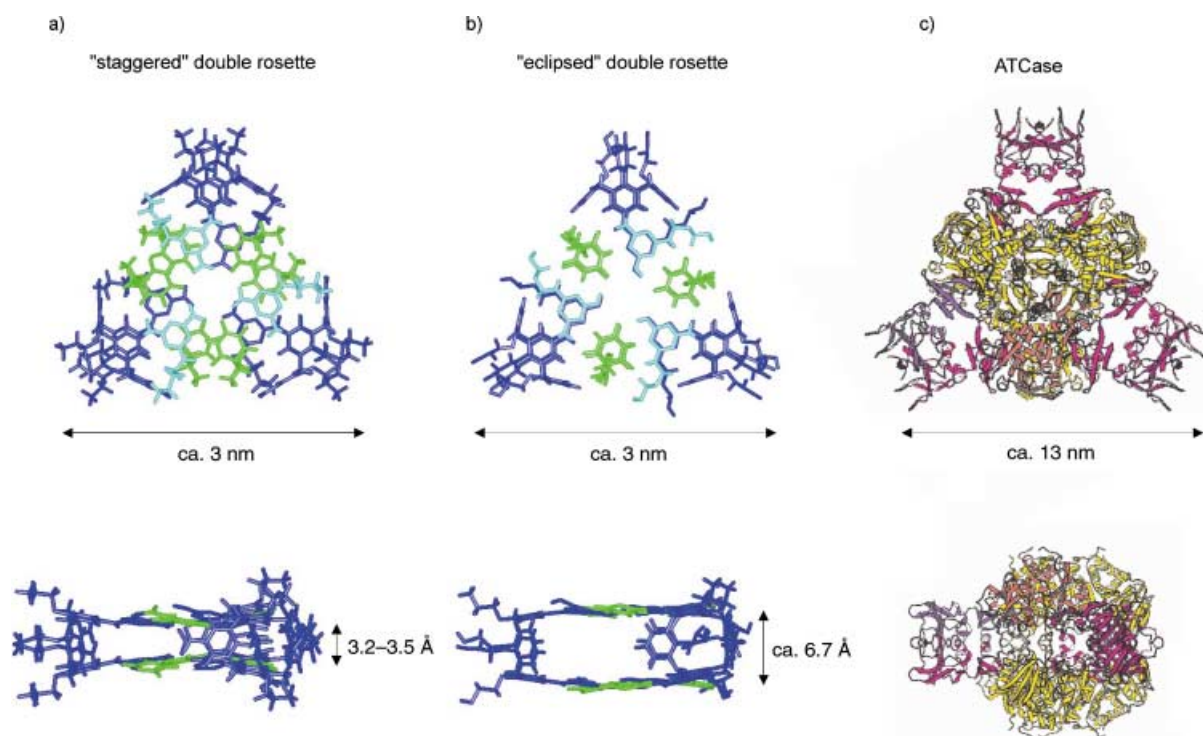


**Figure 3.** a) X-ray crystal structure of double rosette  $1\mathbf{b}_3 \cdot (\text{DEB})_6$  ( $D_3$  symmetry) showing the staggered conformation of the melamine rings. The two melamine rings of each calixarene has been colored differently (dark and light blue) to highlight the staggered orientation). The top view (top) shows the width of the rosette (ca. 3 nm) and the side view (bottom) shows the height of the internal cavity of the structure (ca. 3.2–3.5 Å); b) X-ray crystal structure of complex  $1\mathbf{a}_3 \cdot (\text{DEB})_6 \cdot 2_3$  ( $C_{3h}$  symmetry) showing the eclipsed conformation of the melamine rings (the encapsulated  $2_3$  in the top and side view as well as the ethyl and butyl side chains of the rosettes in the side view are not shown). The top view (top) shows the width of the rosette (ca. 3 nm) and the side view (bottom) shows the height of the internal cavity of the box (ca. 6.4–6.9 Å); c) three-dimensional structure of the natural ATCase enzyme. (Figure 3c is repinted with permission from Ref. [3b].)

(ATCase) are moved apart 12 Å and turned by 10° after binding of *N*-(phosphonacetyl)-L-aspartate and also adopt a more eclipsed position.<sup>[15]</sup> Remarkably, a reduction in symmetry from  $D_3$  to  $C_3$  is also observed in the enzymatic recognition and formation of the complex (Figure 3).<sup>[16]</sup>

In addition, the  $^1\text{H}$  NMR studies shows that the structure of complex  $\mathbf{1a}_3\cdot(\text{DEB})_6\cdot\mathbf{2}_3$  in  $\text{CDCl}_3$  is in full accord with the structure found in the solid state. Furthermore, the solution studies confirm the structural changes proposed from the X-ray analysis. We observed that addition of three equivalents of alizarin **2** to the self-assembled host  $\mathbf{1a}_3\cdot(\text{DEB})_6$ , which has  $D_3$  symmetry,<sup>[17]</sup> resulted in the quantitative self-assembly of a single and highly symmetrical complex in  $\text{CDCl}_3$  (Figure 4). Integration of the signals in the  $^1\text{H}$  NMR spectrum clearly showed a 3:1 complexation of **2** to  $\mathbf{1a}_3\cdot(\text{DEB})_6$ . The presence of only two signals for the barbiturate NH protons confirm the formation of a “super” complex with an eclipsed orientation of the two melamine rings of the calix[4]arene moieties and thus the  $C_{3h}$  symmetry (four signals are expected for the staggered complex,  $C_3$  symmetry). This symmetry implies a change in the spatial disposition of the melamine rings of each calix[4]arene from staggered in the empty assembly to an eclipsed orientation upon complexation of alizarin (Figure 1), as found in the solid state. The titration of  $\mathbf{1a}_3\cdot(\text{DEB})_6$  with 0–3 equivalents of **2** was monitored by  $^1\text{H}$  NMR spectroscopy. The  $^1\text{H}$  NMR spectrum for a  $\mathbf{2}:\mathbf{1a}_3\cdot(\text{DEB})_6$  ratio of less than 3:1 showed the signals corresponding to the  $\mathbf{1a}_3\cdot(\text{DEB})_6\cdot\mathbf{2}_3$  complex as well as the signal for the free  $\mathbf{1a}_3\cdot(\text{DEB})_6$  assembly, thus indicating that slow exchange occurs between the free and complexed assemblies on the NMR timescale. The kinetic stability of the assembly is remarkable; when the sample was heated to 60 °C the  $^1\text{H}$  NMR spectrum still showed the two independent assemblies. Furthermore, separate signals corresponding to free **2** and  $\mathbf{1a}_3\cdot(\text{DEB})_6\cdot\mathbf{2}_3$  could be seen at a  $\mathbf{2}:\mathbf{1a}_3\cdot(\text{DEB})_6$  ratio of 4:1. Significant signals for the intermediates  $\mathbf{1a}_3\cdot(\text{DEB})_6\cdot\mathbf{2}_n$  ( $n=1, 2$ ) were not observed, which indicates that the complexation is strongly cooperative.

2D  $^1\text{H}$  NMR spectroscopic analysis of complex  $\mathbf{1a}_3\cdot(\text{DEB})_6\cdot\mathbf{2}_3$  (1 mM,  $\text{CDCl}_3$ , 298 K) allowed the assignment of the signals in the  $^1\text{H}$  NMR spectrum. The large shifts observed for the alizarin protons ( $\Delta\delta > 3$  ppm) confirmed the encapsulation of the guest molecules in solution. The aromatic protons  $\text{H}_r$ ,  $\text{H}_s$ , and  $\text{H}_t$  of **2** (ring A, see Figure 4) shifted 3.28–3.88 ppm upfield, thus demonstrating that ring A is partially included in the calix[4]arene cone. The observed shift arises from the anisotropy provided by the numerous aromatic rings that line the interior of the cage.<sup>[18]</sup> Many other protons also show very large shifts upon complexation of **2**. For example, the  $\text{NH}_{\text{DEB}}$  protons  $\text{H}_a$  and  $\text{H}_b$  in the complex  $\mathbf{1a}_3\cdot(\text{DEB})_6\cdot\mathbf{2}_3$  are shifted upfield 0.58 ppm and 0.30 ppm, respectively relative to those of the free host  $\mathbf{1a}_3\cdot(\text{DEB})_6$ . Interestingly, the alizarin hydroxy  $\text{OH}_n$  shifts from 6.24 ppm in free **2** to 9.87 ppm ( $\Delta\delta = 3.63$  ppm) in the complex, which suggests that the  $\text{OH}_n$  group is involved in the formation of a hydrogen bond, probably with the carbonyl functionality of an adjacent **2** molecule. The other hydroxy group  $\text{OH}_m$  which is involved in the formation of an intramolecular hydrogen bond before complexation hardly shifted ( $\Delta\delta =$

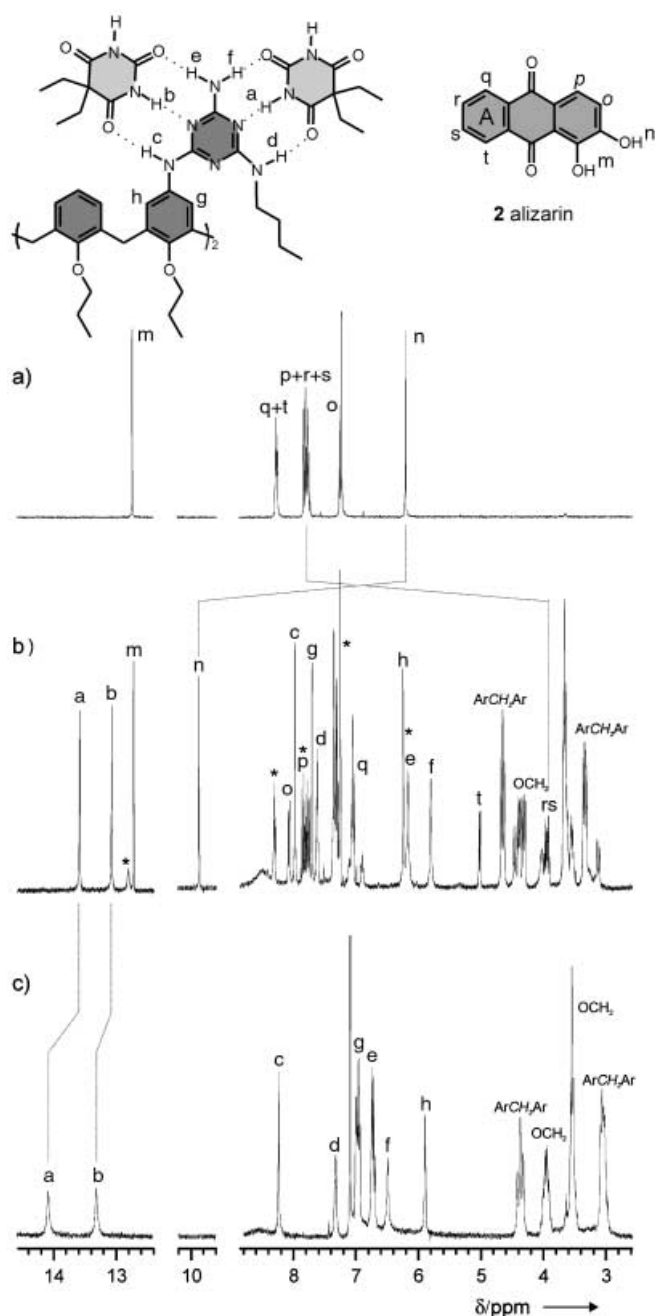


**Figure 4.** Part of the  $^1\text{H}$  NMR spectra (400 MHz, in  $\text{CDCl}_3$  at 298 K relative to residual  $\text{CHCl}_3$ ) of a) guest molecule **2**; b) complex  $\mathbf{1a}_3\cdot(\text{DEB})_6\cdot\mathbf{2}_3$ ; c) assembly  $\mathbf{1a}_3\cdot(\text{DEB})_6$ . Signals marked with \* belong to **2**. The molecular structure of alizarin and part of the double rosette with the corresponding proton assignments are shown.

–0.02 ppm).<sup>[19]</sup> Therefore,  $^1\text{H}$  NMR spectroscopy confirms that the hydrogen-bonded scaffold  $\mathbf{1a}_3\cdot(\text{DEB})_6$  encapsulates the hydrogen-bonded trimer of alizarin (**2**<sub>3</sub>) in between the two rosette layers in a highly organized manner in solution. The structure of the complex  $\mathbf{1a}_3\cdot(\text{DEB})_6\cdot\mathbf{2}_3$  in solution matches exactly that of the X-ray crystal structure, thus confirming the change from the  $D_3$  symmetry of the “empty cage” to the  $C_{3h}$  symmetry of the “filled cage”. In addition, it is important to highlight that the self-assembled template



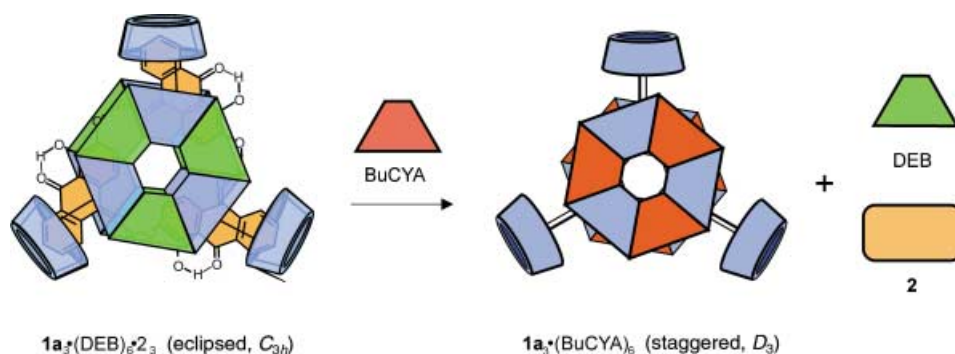


**Figure 5.** Schematic representation of the release of the encapsulated dye trimer  $\mathbf{2}_3$  and the “rearrangement” of the eclipsed to staggered conformation after substitution of the DEB for BuCYA.

$1\mathbf{a}_3 \cdot (\text{DEB})_6$  allows formation of the  $\mathbf{2}_3$  trimer, which is not otherwise observed in solution.

Whereas the common characteristic of all the biological self-assembly systems is the high level of organization of the encapsulated material, specific viruses present another interesting feature, that is, the release of their encapsulated self-assembled genetic material after binding to the wall of a host cell. Also, full control over guest release is of fundamental importance for the development of encapsulation-based applications with synthetic systems.<sup>[20]</sup> The controlled release of the guest in hydrogen-bonded capsules is achieved by pH changes or by the addition of a competitive solvent or molecule, which in all cases results in the breaking of the capsule.<sup>[21]</sup>

We have achieved the release of the encapsulated material from our hydrogen-bonded cage  $1\mathbf{a}_3 \cdot (\text{DEB})_6 \cdot \mathbf{2}_3$  by a specific external molecular recognition stimulus that retains the basic structural topology of the assembly.

Our strategy was based on our previous work where we have shown that barbiturate building blocks (DEB) in assemblies of type  $1\mathbf{a}_3 \cdot (\text{DEB})_6$  can be substituted by cyanurate derivatives (CYA) to form assemblies  $1\mathbf{a}_3 \cdot (\text{CYA})_6$ .<sup>[22]</sup> The barbiturate–cyanurate exchange occurs because cyanurates form much stronger hydrogen bonds with melamines than barbiturates.<sup>[23]</sup>

The controlled addition of butyl cyanurate to the complex  $1\mathbf{a}_3 \cdot (\text{DEB})_6 \cdot \mathbf{2}_3$  releases the encapsulated molecules. This results in an empty self-assembled molecular cage  $1\mathbf{a}_3 \cdot (\text{BuCYA})_6$  and free guest (Figure 5). The release is achieved because assembly  $1\mathbf{a}_3 \cdot (\text{BuCYA})_6$  is not able to template the encapsulation of  $\mathbf{2}_3$  because of the different geometry of the cyanurates compared to that of the barbiturates.<sup>[24]</sup>

The release of the encapsulated guest has been studied by  $^1\text{H}$  NMR spectroscopy. The addition of 2.1 equivalents of BuCYA to the  $C_{3h}$ -symmetric complex  $1\mathbf{a}_3 \cdot (\text{DEB})_6 \cdot \mathbf{2}_3$  showed that all the signals of  $1\mathbf{a}_3 \cdot (\text{DEB})_6 \cdot \mathbf{2}_3$  had disappeared from the  $^1\text{H}$  NMR spectrum and that only signals corresponding to assembly  $1\mathbf{a}_3 \cdot (\text{BuCYA})_6$ , free  $\mathbf{2}$ , and free DEB were present. NMR spectroscopic analysis also revealed a structural rearrangement of the melamine calix[4]arene derivative from a staggered to an eclipsed conformation of the melamines.<sup>[25]</sup> This reorganization results in the empty assembly  $1\mathbf{a}_3 \cdot (\text{BuCYA})_6$  formed after the release of  $\mathbf{2}_3$  having  $D_3$  symmetry.

Thus, we have now achieved a high control over the self-organization process. The work presented here compiles in a single system many separated supramolecular strategies that chemists have used over the last three decades to master the molecular self-assembly process. We have designed building blocks that not only show a strong affinity for each other and form a predictable self-assembled molecular cage with self-assembled encapsulated material, but which display topological and regulatory strategies similar to those found in nature that allow functions such as templating and guest release.

Received: August 28, 2003 [Z52733]

Published Online: November 11, 2003

**Keywords:** enzyme mimics · host–guest systems · hydrogen bonds · receptors · self-assembly

- [1] Special Issue “Supramolecular Chemistry and Self-Assembly”: *Science* **2002**, 295, 2400–2421.
- [2] a) N. C. Seeman, A. M. Belcher, *Proc. Natl. Acad. Sci. USA* **2002**, 99, 6451–6455; b) Special Issue “Nanostructures”: E. A. Chandross, R. D. Miller, *Chem. Rev.* **1999**, 99, 1644–1990.
- [3] J. S. Lindsey, *New J. Chem.* **1991**, 15, 153–180; b) L. Stryer, *Biochemistry*, 4th ed, Freeman and Company, New York, **1995**.
- [4] M. Lyndsey, D. Philp, *Chem. Soc. Rev.* **2001**, 30, 287–302.
- [5] R. Fiammengo, M. Crego-Calama, D. N. Reinhoudt, *Curr. Opin. Chem. Biol.* **2001**, 5, 660–673.
- [6] a) M. M. Conn, J. Rebek, Jr., *Chem. Rev.* **1997**, 97, 1647–1668; b) F. Hof, S. L. Craig, C. Nuckolls, J. Rebek, Jr., *Angew. Chem.* **2002**, 114, 1556–1578; *Angew. Chem. Int. Ed.* **2002**, 41, 1488–1508, and references therein; c) C. A. Schalley, *Angew. Chem.* **2002**, 114, 1583–1586; *Angew. Chem. Int. Ed.* **2002**, 41, 1513–1515, and references therein.
- [7] a) J. Kang, J. Rebek, Jr., *Nature* **1996**, 382, 239–241; b) T. Heinz, D. M. Rudkevich, J. Rebek, Jr., *Nature* **1998**, 394, 764–766; c) T. Kusukawa, M. Fujita, *J. Am. Chem. Soc.* **2002**, 124, 13576–13582; d) M. Ziegler, J. L. Brumaghim, K. N. Raymond, *Angew. Chem.* **2000**, 112, 4285–4287; *Angew. Chem. Int. Ed.* **2000**, 39, 4119–4121.
- [8] J.-M. Lehn, *Science* **2002**, 295, 2400–2403.
- [9] L. J. Prins, D. N. Reinhoudt, P. Timmerman, *Angew. Chem.* **2001**, 113, 2446–2492; *Angew. Chem. Int. Ed.* **2001**, 40, 2382–2426.
- [10] C. T. Seto, G. M. Whitesides, *J. Am. Chem. Soc.* **1993**, 115, 905–916.
- [11] a) P. Timmerman, R. H. Vreekamp, R. Hulst, W. Verboom, D. N. Reinhoudt, K. Rissanen, K. A. Udachin, J. Ripmeester, *Chem. Eur. J.* **1997**, 3, 1823–1832; b) R. H. Vreekamp, J. P. M. Van

- Duynhoven, M. Hubert, W. Verboom, D. N. Reinhoudt, *Angew. Chem.* **1996**, *108*, 1306–1309; *Angew. Chem. Int. Ed. Engl.* **1996**, *35*, 1215–1218.
- [12] P. Timmerman, D. N. Reinhoudt, *Adv. Mater.* **1999**, *11*, 71–74.
- [13] A crystal of **1a**<sub>3</sub>(DEB)<sub>6</sub>**2**<sub>3</sub> with dimensions 0.25 × 0.25 × 0.25 mm was placed on a Lindemann glass capillary and placed in the cold nitrogen stream ( $T = 150$  K) of a Nonius KappaCCD diffractometer ( $\lambda_{\text{MoK}\alpha} = 0.71073$  Å). Crystal data: cubic,  $P\bar{a}3$  (no. 205),  $a = 41.043(6)$  Å,  $V = 69138(18)$  Å<sup>3</sup>,  $Z = 8$ , no absorption correction was applied. The structure was solved by direct methods (SHELXS97). 35% of the unit cell is filled with disordered solvent molecules, which were incorporated in the model with the PLATON/SQUEEZE procedure. A total of 5360 electrons was found in the disordered solvent region. Some butyl and propyl moieties, which bordered the disordered solvent region, displayed disorder, which could be described with a two-site model. 186112 reflections were measured,  $\theta_{\text{max}} = 21.05^\circ$ , of which 12481 were unique, and 1009 parameters refined. Final  $wR2 = 0.2551$ ,  $R1 = 0.0899$ ,  $S = 1.053$ , min./max. residual density =  $-0.30/0.43$  e Å<sup>-3</sup>. CCDC-218142 contains the supplementary crystallographic data for this paper. These data can be obtained free of charge via [www.ccdc.cam.ac.uk/conts/retrieving.html](http://www.ccdc.cam.ac.uk/conts/retrieving.html) (or from the Cambridge Crystallographic Data Centre, 12 Union Road, Cambridge CB2 1EZ, UK; fax: (+44) 1223-336-033; or deposit@ccdc.cam.ac.uk).
- [14] Other interactions such as van der Waals, attractive electrostatic, and interactions between hydrogen-bonding arrays and aromatic or heteroaromatic rings may play a role. a) E. A. Meyer, R. K. Castellano, F. Diederich, *Angew. Chem.* **2003**, *115*, 1244–1287; *Angew. Chem. Int. Ed.* **2003**, *42*, 1210–1250; b) C. A. Hunter, J. K. M. Sanders, *J. Am. Chem. Soc.* **1990**, *112*, 5525–5534; c) C. A. Hunter, *Chem. Soc. Rev.* **1994**, *23*, 101–109.
- [15] K. L. Krause, K. W. Volz, W. N. Lipscomb, *Proc. Natl. Acad. Sci. USA* **1985**, *82*, 1643–1647.
- [16] A  $C_3$  symmetry would also be obtained for our complex if the building blocks were chiral.
- [17] L. J. Prins, J. Huskens, F. De Jong, P. Timmerman, D. N. Reinhoudt, *Nature* **1999**, *398*, 498–502.
- [18] S. Saito, C. Nuckolls, J. Rebek, Jr., *J. Am. Chem. Soc.* **2000**, *122*, 9628–9630.
- [19] NOE connectivities between OH<sub>n</sub> and H<sub>q</sub> of the same molecule **2** and between OH<sub>n</sub> and H<sub>o</sub> of the neighboring molecule **2** can be seen in the 2D NMR spectrum. The last connectivity is only possible if the OH groups in the trimer **2**<sub>3</sub> are pointing outwards (for assignment of the protons see Figure 2).
- [20] a) K. Park, *Controlled Drug Delivery: Challenges and Strategies*, American Chemical Society, Washington DC, **1997**; b) T. Douglas, M. Young, *Nature* **1998**, *393*, 152–155; c) N. K. Mal, M. Fujiwara, Y. Tanaka, *Nature* **2003**, *421*, 350–353.
- [21] a) S. K. Körner, F. C. Tucci, D. M. Rudkevich, T. Heinz, J. Rebek, Jr., *Chem. Eur. J.* **2000**, *6*, 187–195; b) B. C. Hamann, K. D. Shimizu, J. Rebek, Jr., *Angew. Chem.* **1996**, *108*, 1425–1427; *Angew. Chem. Int. Ed. Engl.* **1996**, *35*, 1326–1329; c) N. Branda, R. M. Grotzfeld, C. Valdés, J. Rebek, Jr., *J. Am. Chem. Soc.* **1995**, *117*, 85–88.
- [22] L. J. Prins, F. De Jong, P. Timmerman, D. N. Reinhoudt, *Nature* **2000**, *408*, 181–184.
- [23] A. G. Bielejewska, C. E. Marjo, L. J. Prins, P. Timmerman, F. De Jong, D. N. Reinhoudt, *J. Am. Chem. Soc.* **2001**, *123*, 7518–7533.
- [24] Somehow the structure of DEB, with its tetrahedral sp<sup>3</sup> carbon atom, allows a better fit for the **2** trimer than CYA with its flatter sp<sup>3</sup> nitrogen atom.
- [25] L. J. Prins, K. A. Jolliffe, R. Hulst, P. Timmerman, D. N. Reinhoudt, *J. Am. Chem. Soc.* **2000**, *122*, 3617–3627.